Clinical Biomechanics 37 (2016) 153–159

Contents lists available at ScienceDirect

Clinical Biomechanics

journal homepage: www.elsevier.com/locate/clinbiomech

A biologically-assisted curved muscle model of the lumbar spine: Model validation

Jaejin Hwang [a], Gregory G. Knapik [a], Jonathan S. Dufour [a], Thomas M. Best [a,b], Safdar N. Khan [a,c], Ehud Mendel [a,d], William S. Marras [a,*]

[a] Biodynamics Laboratory, Spine Research Institute, Department of Integrated Systems Engineering, The Ohio State University, 210 Baker Systems Engineering, 1971 Neil Avenue, Columbus, OH 43210, USA
[b] Department of Family Medicine, The Ohio State University, Martha Moorehouse Medical Plaza, 2050 Kenny Dr., Columbus, OH 43210, USA
[c] Department of Orthopaedics, College of Medicine, The Ohio State University, Columbus, OH 43210, USA
[d] Department of Neurological Surgery, The Ohio State University, Columbus, OH 43210, USA

ARTICLE INFO

Article history:
Received 21 March 2016
Accepted 26 July 2016

Keywords:
Curved muscle
Wrapping muscle
Biomechanical model
Validation
Spine

ABSTRACT

Background: Biomechanical models have been developed to predict spinal loads *in vivo* to assess potential risk of injury in workplaces. Most models represent trunk muscles with straight-lines. Even though straight-line muscles behave reasonably well in simple exertions, they could be less reliable during complex dynamic exertions. A curved muscle representation was developed to overcome this issue. However, most curved muscle models have not been validated during dynamic exertions. Thus, the objective of this study was to investigate the fidelity of a curved muscle model during complex dynamic lifting tasks, and to investigate the changes in spine tissue loads.

Methods: Twelve subjects (7 males and 5 females) participated in this study. Subjects performed lifting tasks as a function of load weight, load origin, and load height to simulate complex exertions. Moment matching measures were recorded to evaluate how well the model predicted spinal moments compared to measured spinal moments from T12/L1 to L5/S1 levels.

Findings: The biologically-assisted curved muscle model demonstrated better model performance than the straight-line muscle model between various experimental conditions. In general, the curved muscle model predicted at least 80% of the variability in spinal moments, and less than 15% of average absolute error across levels. The model predicted that the compression and anterior–posterior shear load significantly increased as trunk flexion increased, whereas the lateral shear load significantly increased as trunk twisted more asymmetric during lifting tasks.

Interpretation: A curved muscle representation in a biologically-assisted model is an empirically reasonable approach to accurately predict spinal moments and spinal tissue loads of the lumbar spine.

1. Introduction

In a companion paper (Hwang et al., 2016b), the model structure that includes curved torso muscle paths with its underlying logic for a biologically-assisted model of the lumbar spine is described. This model is believed to overcome the limitations of historical straight-line muscle model approaches that are particularly relevant for complex, multi-plane exertions. However, the model fidelity associated with predictions of spinal moments and spinal tissue loads at multiple disc levels in this curved muscle model had not been evaluated. Thus, the first objective of this study was to evaluate the robustness and performance of a biologically-assisted curved muscle model compared to a previous straight-line muscle model during complex dynamic lifting tasks. The second objective of this study was to investigate the effect of external loads and complex lumbar motions on spine tissue loads of a curved muscle model.

2. Methods

2.1. Participants

Following IRB informed consent, twelve subjects (7 male, 5 female) participated in this study. All subjects had no prior history of low back pain that caused them to seek medical attention. Mean values and standard deviations of age, body mass, and stature of all subjects were 26.9 (4.3) years, 70.8 (15.3) kg, and 173.5 (10.2) cm, respectively.

* Corresponding author.
E-mail addresses: hwang.285@osu.edu (J. Hwang), knapik.1@osu.edu (G.G. Knapik), dufour.8@osu.edu (J.S. Dufour), Tom.Best@osumc.edu (T.M. Best), Safdar.Khan@osumc.edu (S.N. Khan), Ehud.Mendel@osumc.edu (E. Mendel), marras.1@osu.edu (W.S. Marras).

http://dx.doi.org/10.1016/j.clinbiomech.2016.07.009
0268-0033/

2.2. Instrumentation

Muscle activities were collected via surface electrodes (Motion Lab Systems MA300-XVI, Baton Rouge, Louisiana, USA) over ten trunk muscles. An OptiTrack optical motion capture system (NaturalPoint, Corvallis, OR, USA) with 24 Flex 3 infrared cameras was used to monitor trunk kinematics. A Bertec 4060A force plate (Bertec, Worthington, OH, USA) was used to measure ground reaction forces. Customized Laboratory software and a data acquisition system (NI USB-6225, National Instruments, Austin, TX, USA) were used to collect all signals simultaneously and efficiently run the biomechanical model.

2.3. Testing procedure

Surface electrodes were placed over ten trunk muscles including the right and left pairs of the latissimus dorsi (most lateral portion of the muscle at the T9 level), erector spinae (approximately 4 cm apart from midline of spine at the L3 level), rectus abdominus (3 cm from the midline of the abdomen, and 2 cm above the umbilicus), internal obliques (4 cm above ilium in the lumbar triangle at 45° to the midline of the spine) and external obliques (10 cm from the midline of the abdomen and 4 cm above the ilium at 45° to the midline of the abdomen) based on standard placement guidelines (Mirka and Marras, 1993). Forty-one reflective markers were attached to each subject's body according to the baseline marker set in Optitrack's Motive software (http://www.optitrack.com).

Calibration exertions were performed by each subject to optimize the physiological properties for each of the ten trunk muscles. Subjects were required to stand on two force plates and perform concentric and eccentric lumbar exertions in multiple planes with a 9.1 kg weight. They were instructed to perform within a comfortable range of motion and speed, and repeat the procedure three times. These exertions encouraged dynamic ranges of muscle length, muscle velocity and muscle activities for each person. The experimenter explained the multi-planar concentric and eccentric exertions to subjects and allowed them to become familiar with it before recording the tasks.

For the independent test set, subjects were required to lift a weighed box with handles as a function of different load weights (6.8 kg and 13.6 kg), load origins (counterclockwise 60°, counterclockwise 30°, 0°, clockwise 30°, and clockwise 60°), and load heights (ankle, knee, and waist) with a total of two repetitions for each experimental combination. The order of load height was randomly counterbalanced across subjects, and the order of load weights and load origins were fully randomized. Subjects were allowed to bend their knees during lifting and each task was started from an upright posture and finished in an upright posture holding the box. Subjects were instructed to perform the lift at a comfortable speed. The duration of each task was typically less than 10 s. In order to protect the subjects, only symmetric lifting was performed at the ankle height conditions. A total of 44 trials of various lifting conditions were performed by each subject.

2.4. Data analysis

For model fidelity measures, a comparison of muscle-generated predicted moments and externally measured moments was performed in sagittal and lateral planes from T12/L1 to L5/S1 levels. A multi-planar (sagittal and lateral planes) weighted squared correlation coefficient (R^2) and average absolute error (AAE) measurement was used to describe performance. The R^2 coefficient indicates the amount of variability accounted for by comparing external and internal spinal moment curves in each physiological plane. The AAE (%) represents the overall average magnitude of absolute error between external and internal spinal moments normalized relative to the peak external moment in each physiological plane. The peak absolute three-dimensional spinal tissue loads including compression, anterior–posterior shear, and lateral shear were evaluated at the superior endplate of each lumbar disc level.

2.5. Statistical analysis

Univariate analysis of variance (ANOVA) with a significance level 0.05 was conducted. Independent variables were the load weight, load origin, and load height. Dependent variables were peak three-dimensional spinal loads. Main effects and interactions of load weight, load origin, and load height on spinal loads were evaluated, and subject was treated as a blocking factor.

3. Results

After calibration, mean and standard deviations of gain and gain ratio were 58.2 (22.1) N/cm^2 and 28.8 (12.7) N/cm^2 V, respectively. The ten muscle gains across all twelve subjects ranged from 34.0 N/cm^2 to 99.8 N/cm^2, and 10 gain ratios ranged from 11.6 N/cm^2 V to 61.1 N/cm^2 V.

In terms of model performance during complex dynamic multi-planar lifting, Fig. 1 shows the direct comparison of model fidelity measures between the curved muscle model and a straight-line muscle model during complex dynamic lifting tasks. The curved muscle model generally showed a better model performance than the straight-line muscle model of the lumbar spine. The overall multi-planar R^2 and AAE of the curved muscle model were 0.84 and 13% whereas the straight-line muscle model showed 0.78 and 20%. The curved muscle model normally showed a consistent model performance across multiple levels whereas the straight-line muscle model showed much worse performance above L2/L3 disc level. For example, at T12/L1 level, the AAE (%) of the curved muscle model was less than half of the straight-line muscle model (16% vs. 37%).

Since the curved muscle model showed much better performance than the straight-line muscle model, a more in depth analysis was conducted specifically for the curved muscle model. Table 1 shows the summary of mean and standard deviations of multi-planar (resultant moment) average R^2 and normalized AAE for all disc levels by the interaction between the load origin and load height. During the lifting from any conditions between various heights and load origins, the multi-planar average R^2 of all levels was greater than 0.8 (ranged from 0.8 to 0.86) and AAE was less than 15% (ranged from 11.69% to 14.07%). For the lifting from knee height, the differences of R^2 and AAE of all levels between various load origins were up to 0.02 and 2.38%, respectively. Lifting from waist height showed the difference of R^2 and AAE of all levels between load origins up to 0.02 and 0.7%, respectively.

Table 2 shows main effects and two-way interactions of three-dimensional spine tissue loads. There were differences for peak compression, peak anterior–posterior shear, and peak lateral shear load by load weight, load origin, and load height for most levels. No statistically significant differences in peak anterior–posterior shear load at L4/L5 ($P = 0.55$) by load weight, and L1/L2 ($P = 0.07$) and L3/L4 ($P = 0.09$) by load origin were present (Table 2).

The three-dimensional spinal loads were greater when lifting a heavier box. Lifting a 13.6 kg box from ankle height showed the highest peak compression at L3/L4 (3442 N), the highest peak anterior–posterior shear at L5/S1 (715 N), and the peak lateral shear at L5/S1 (111 N). Fig. 2 shows an example of the peak compression at various disc levels as a function of load weight. Three-dimensional spinal loads increased as the load height decreased. Symmetric lifting from ankle height showed the highest peak compression at L3/L4 (3279 N), the highest peak anterior–posterior shear at L5/S1 (709 N), and the highest peak lateral shear at L5/S1 (104 N). Fig. 3 shows an example of the peak anterior–posterior shear loads at the various disc levels as a function of load height. Increasing load origin substantially increased the peak lateral shear loads, and lifting from counterclockwise 60° showed the highest peak lateral shear load at L5/S1 (242 N). Fig. 4 showed the peak lateral shear load at the various disc levels as a function of the load origin.

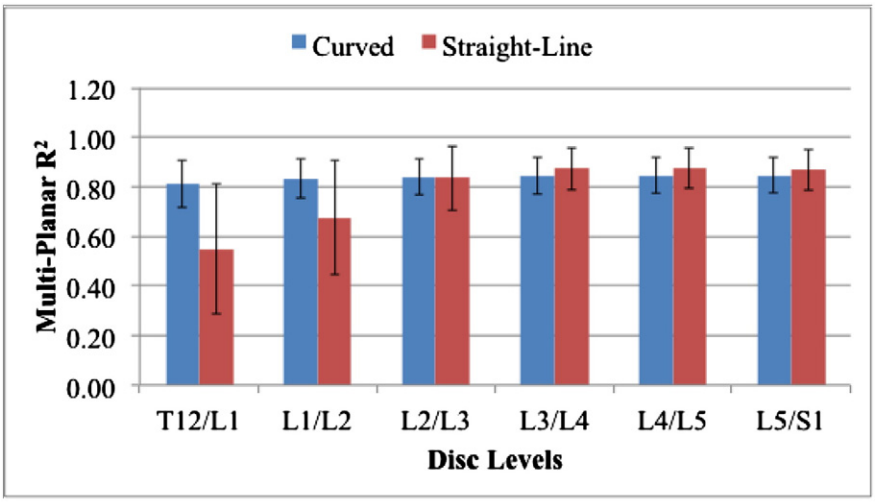

(a)

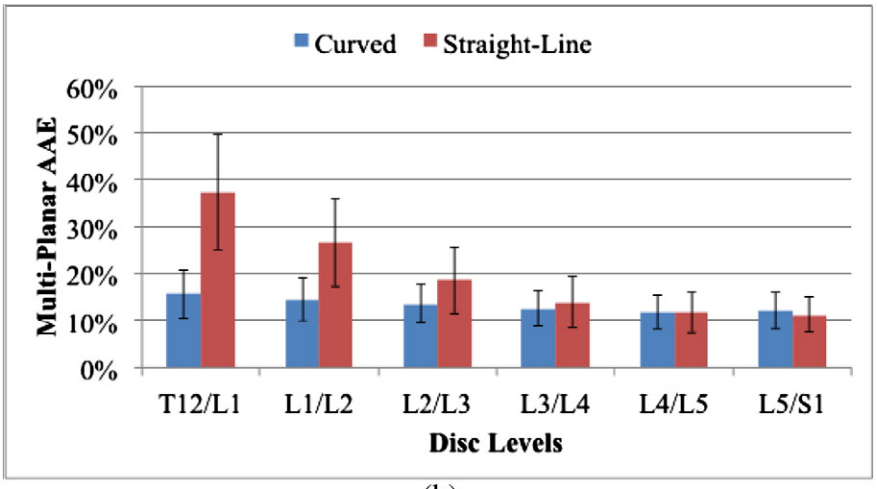

(b)

Fig. 1. Comparison of multi-planar R^2 (a) and average absolute error (AAE) (b) between the curved muscle model and the straight-line muscle model during complex lifting tasks.

Statistically significant interactions between load weight and load origin existed for peak compression at all levels, peak anterior–posterior shear at L2/L3 and L5/S1, and peak lateral shear at all levels except T12/L1 (Table 2). Load weight and load height showed significant interactions for peak compression at all levels except L5/S1, peak anterior–posterior shear at L3/L4 and L5/S1, and peak lateral shear at all levels (Table 2). Interactions between load origin and load height showed statistically significant differences for peak anterior–posterior shear load at T12/L1 through L2/L3, and peak lateral shear at T12/L1 and L3/L4 through L5/S1 (Table 2).

4. Discussion

The biologically-assisted curved muscle model evaluated in this effort showed much better model performance than the straight-line muscle model specifically at upper levels of the lumbar spine. In addition, the curved muscle model showed repeatable model fidelity between various conditions of dynamic lifting tasks. The overall lack of significant differences for model performance measures between experimental conditions indicated the curved muscle model's robust fidelity. In general, the model performed extremely well over a large range of complex dynamic motions and could account for at least 80% of the variability in multi-planar spinal moments from level to level in any interactions between various load origins and load heights. The model could normally predict spinal moments with less than 15% average error from level to level. The differences for multi-planar average R^2 and AAE between main effects (load weight, load origin, and load height) of all levels were only around 0.03 and 1.17%. Given the complex exertions examined in this study, including deep bending and highly asymmetric lifting, it was considered that the model demonstrated quite acceptable performance.

The curved muscle model showed significantly different performance than the straight-line muscle model especially at the higher levels of the lumbar spine. This could be related to the amount of curvatures of trunk muscles at different levels. Table 3 showed the spinal loads distributions at multiple levels of curved and straight-line muscle models during complex lifting tasks. At the upper levels of the lumbar spine, the difference in the three-dimensional spinal loads between the two models were the greatest, most likely due to the fact that muscles at this level had more curvature, which could significantly improve the performance of the curved muscle model. However, it should also be pointed out that significant differences in load trade-offs also occurred at the lower levels. Some differences in spine loads were as large as 58% from L3/L4 and below between models. In general, this study has indicated that curved characteristics of trunk muscles provide additional loading insight compared to straight-line muscles.

In order to appreciate the effects of the curved muscle model's improvements, we compared it's performance to previous versions of the

Table 1
Mean (standard deviations) of multi-planar R^2 and AAE (%) as a function of the load origin and load height.

Disc levels	Load height	R^2					AAE (%)				
		CCW 60°	CCW 30°	0°	CW 30°	CW 60°	CCW 60°	CCW 30°	0°	CW 30°	CW 60°
T12/L1	Ankle			0.76 (0.10)					16.87 (6.05)		
	Knee	0.83 (0.12)	0.83 (0.13)	0.82 (0.09)	0.83 (0.11)	0.83 (0.10)	18.03 (6.62)	14.76 (5.67)	13.12 (4.31)	15.41 (4.92)	17.86 (4.06)
	Waist	0.82 (0.07)	0.81 (0.06)	0.81 (0.07)	0.81 (0.06)	0.79 (0.10)	15.24 (4.21)	14.84 (4.64)	14.31 (5.33)	14.59 (3.81)	16.28 (4.68)
L1/L2	Ankle			0.79 (0.09)					15.46 (5.40)		
	Knee	0.85 (0.09)	0.85 (0.10)	0.83 (0.07)	0.85 (0.08)	0.86 (0.08)	16.47 (5.58)	13.73 (4.83)	12.20 (3.21)	14.04 (3.93)	16.11 (3.34)
	Waist	0.83 (0.07)	0.83 (0.06)	0.82 (0.07)	0.82 (0.06)	0.81 (0.09)	14.10 (3.97)	13.93 (4.28)	13.66 (5.12)	13.72 (3.71)	14.92 (4.21)
L2/L3	Ankle			0.81 (0.08)					14.59 (5.00)		
	Knee	0.86 (0.09)	0.86 (0.08)	0.84 (0.07)	0.86 (0.07)	0.87 (0.07)	14.83 (4.93)	12.83 (4.16)	11.78 (2.81)	12.99 (3.31)	14.56 (2.82)
	Waist	0.84 (0.07)	0.84 (0.06)	0.82 (0.07)	0.83 (0.06)	0.82 (0.07)	13.22 (3.78)	13.33 (4.07)	13.30 (5.06)	13.15 (3.59)	13.77 (3.94)
L3/L4	Ankle			0.82 (0.09)					13.56 (4.44)		
	Knee	0.87 (0.09)	0.86 (0.08)	0.84 (0.08)	0.86 (0.07)	0.87 (0.07)	12.80 (4.21)	11.75 (3.69)	11.35 (2.57)	11.95 (2.96)	12.72 (2.47)
	Waist	0.84 (0.07)	0.84 (0.06)	0.83 (0.07)	0.83 (0.05)	0.83 (0.07)	12.57 (3.52)	12.83 (3.95)	13.01 (5.02)	12.69 (3.57)	12.87 (3.95)
L4/L5	Ankle			0.82 (0.09)					12.18 (3.71)		
	Knee	0.88 (0.08)	0.87 (0.07)	0.84 (0.08)	0.86 (0.07)	0.88 (0.07)	10.95 (3.01)	10.64 (3.12)	10.73 (2.39)	10.88 (2.95)	10.72 (2.58)
	Waist	0.84 (0.07)	0.84 (0.06)	0.83 (0.07)	0.83 (0.05)	0.83 (0.06)	12.26 (3.51)	12.52 (4.17)	12.65 (4.87)	12.24 (3.74)	12.34 (4.06)
L5/S1	Ankle			0.82 (0.08)					10.89 (3.16)		
	Knee	0.88 (0.07)	0.87 (0.07)	0.85 (0.07)	0.87 (0.07)	0.88 (0.07)	11.36 (2.79)	11.10 (2.97)	10.98 (2.67)	11.29 (3.49)	10.67 (3.47)
	Waist	0.84 (0.07)	0.83 (0.06)	0.83 (0.07)	0.83 (0.05)	0.83 (0.07)	13.70 (3.95)	13.71 (4.72)	13.35 (4.75)	13.03 (4.14)	13.47 (4.44)
Average (all levels)	Ankle			0.80 (0.03)					13.92 (2.19)		
	Knee	0.86 (0.02)	0.86 (0.02)	0.84 (0.01)	0.85 (0.01)	0.86 (0.02)	14.07 (2.85)	12.47 (1.60)	11.69 (0.88)	12.76 (1.74)	13.77 (2.93)
	Waist	0.84 (0.01)	0.83 (0.01)	0.82 (0.01)	0.82 (0.01)	0.82 (0.02)	13.51 (1.09)	13.53 (0.83)	13.38 (0.57)	13.24 (0.83)	13.94 (1.44)

Note: Two levels of load weights were pooled. Only symmetric lifting was performed at ankle height. AAE = average absolute error; CCW = counter clockwise; CW = clockwise.

Table 2
Summary of statistically significant main effects and two-way interactions of spinal loads (*P*-values).

Disc levels	Measures	Load weight	Load origin	Load height	Load weight × load origin	Load weight × load height	Load origin × load height
T12/L1	COMP (N)	0.0016*	0.0001*	<.0001*	0.0088*	0.0411*	0.9354
	AP (N)	0.0003*	0.0401*	0.0001*	0.0617	0.2126	0.0020*
	LAT (N)	0.0027*	<.0001*	<.0001*	0.1594	0.0004*	0.0019*
L1/L2	COMP (N)	0.0017*	0.0001*	<.0001*	0.0087*	0.0419*	0.9191
	AP (N)	0.0002*	0.0731	0.0002*	0.0739	0.1152	0.0008*
	LAT (N)	0.0009*	<.0001*	0.0007*	0.0084*	0.0024*	0.4884
L2/L3	COMP (N)	0.0018*	0.0002*	<.0001*	0.0094*	0.0438*	0.9256
	AP (N)	0.0002*	0.0456*	<.0001*	0.0442*	0.0843	0.0155*
	LAT (N)	0.0018*	<.0001*	<.0001*	0.0047*	0.0072*	0.0991
L3/L4	COMP (N)	0.0019*	0.0002*	<.0001*	0.0101*	0.0475*	0.9361
	AP (N)	0.0354*	0.0875	<.0001*	0.0942	0.0004*	0.2430
	LAT (N)	0.0014*	<.0001*	<.0001*	0.0053*	0.0096*	0.0487*
L4/L5	COMP (N)	0.0019*	0.0002*	<.0001*	0.0109*	0.0489*	0.9445
	AP (N)	0.5536	0.0373*	<.0001*	0.3123	0.2303	0.2860
	LAT (N)	0.0029*	<.0001*	<.0001*	0.0077*	0.0263*	0.0049*
L5/S1	COMP (N)	0.0020*	0.0002*	<.0001*	0.0120*	0.0528	0.9470
	AP (N)	0.0120*	0.0001*	<.0001*	0.0380*	0.0093*	0.6571
	LAT (N)	0.0048*	<.0001*	<.0001*	0.0152*	0.0482*	0.0005*

Note: COMP = compression; AP = anterior–posterior shear; LAT = lateral shear.
* *P*-values < 0.05.

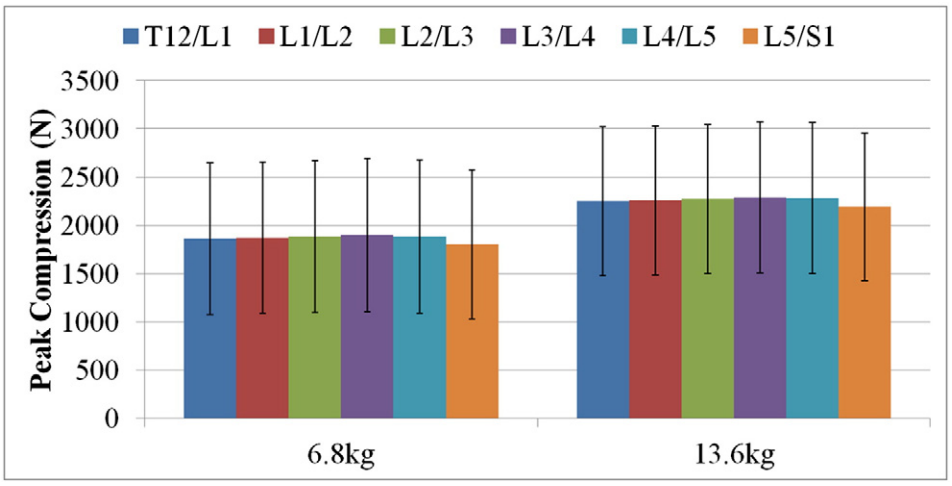

Fig. 2. Peak compression at various disc levels as a function of load weight.

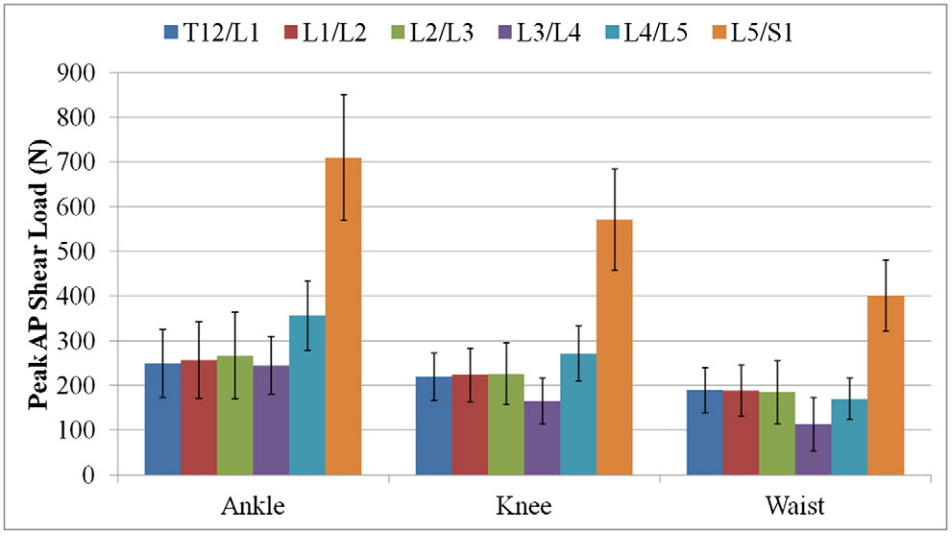

Fig. 3. Peak anterior–posterior (AP) shear load at various disc levels as a function of load height. Only symmetric lifting is shown.

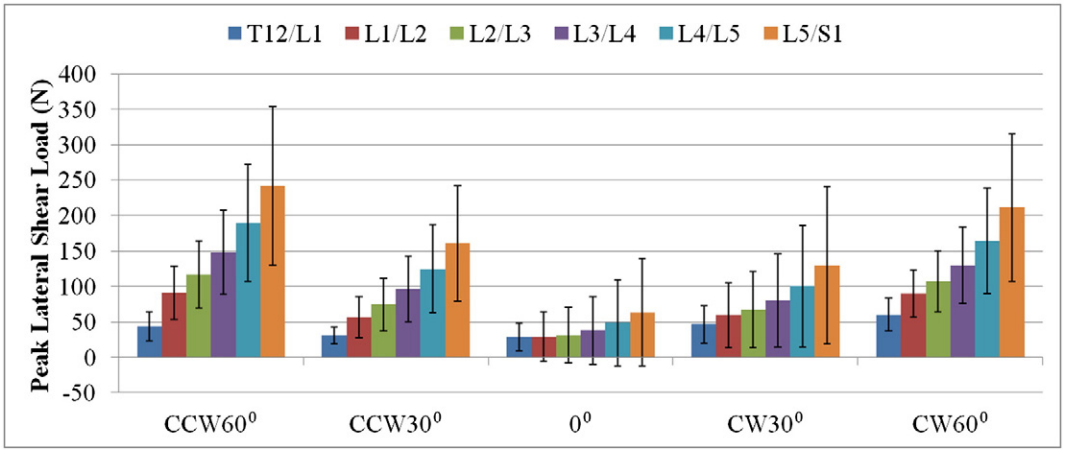

Fig. 4. Peak lateral shear load at various disc levels as a function of load origin. CCW = counterclockwise; CW = clockwise. Ankle symmetric lifting is not included in this figure.

Table 3
Comparison of average three-dimensional spinal loads at multiple levels between the curved muscle model and the straight-line muscle model.

Disc levels	Measures	Curved	Straight-line	Difference
T12/L1	COMP (N)	2056	1718	20%
	AP (N)	206	810	−75%
	LAT (N)	42	285	−85%
L1/L2	COMP (N)	2065	1783	16%
	AP (N)	208	698	−70%
	LAT (N)	63	265	−76%
L2/L3	COMP (N)	2077	1847	12%
	AP (N)	207	548	−62%
	LAT (N)	77	225	−66%
L3/L4	COMP (N)	2093	1906	10%
	AP (N)	145	342	−58%
	LAT (N)	95	176	−46%
L4/L5	COMP (N)	2083	1932	8%
	AP (N)	228	259	−12%
	LAT (N)	121	141	−14%
L5/S1	COMP (N)	1996	1869	7%
	AP (N)	494	607	−19%
	LAT (N)	156	113	38%

Note: Difference = (Curved − Straight-Line) / Straight-Line. Average spinal loads of all lifting tasks were summarized.

model. Previous straight-line muscle models have reported the sagittal plane R^2 ranged from 0.65 to 0.89 at L5/S1 level during constrained sagittal bending (Granata and Marras, 1993; Marras and Sommerich, 1991), constrained sagittal lifting (Granata and Marras, 1995), whole body free-dynamic sagittal and asymmetric lifting (Marras and Granata, 1997), and sagittal pushing, pulling, and lifting (Theado et al., 2007). However, most of these approaches were only validated for sagittal lifting from knee height. Only one study (Granata and Marras, 1995) considered the 30 degree of load origin, and sagittal plane R^2 and AAE were 0.81 and 17.5 N m, respectively. Given the complex whole body free-dynamic lifting conditions including ankle to waist height and 60 degree of load origin, the current curved muscle model showed the sagittal plane R^2 and AAE as 0.87 and 11.71 N m across all disc levels, respectively. The improved performance and stability of the model were evident through a broad range of trunk motions during complex dynamic lifting tasks.

In the present study, multi-planar weighted model fidelity measures rather than single-planar measures were used as a performance indicator. For instance, lateral plane moments were negligible compared to sagittal moments during primary sagittal lifting. However, it could be misinterpreted as low performance for the lateral plane given the low lateral plane R^2 values. In order to overcome this, summation of single-planar measures (sagittal and lateral planes) were weighted relative to peak in-plane external moments, thus giving more significance to the planes of the body that experience more significant loads. The functional validity of this measure was empirically tested in a previous study (Dufour et al., 2013).

The curved muscle model necessitated an increased level of complexity in terms of anatomical muscle parameters such as descriptions of the muscle moment-arms and muscle physiological cross-sectional areas at multiple levels of the thoracic/lumbar spine. The polynomial regression model was previously developed based on 30 subjects (20 females and 10 males) from MRI-database (Jorgensen et al., 2001; Marras et al., 2001). The predictive regression model generally demonstrated improved predictability compared to previous studies (Anderson et al., 2012; Chaffin et al., 1990; Moga et al., 1993; Seo et al., 2003). In addition, the developed regression models were applied to a new subject group (7 males and 5 females) in this study, and the predicted muscle parameters indicated a comparable muscle geometric pattern with an historical dataset. These results suggest very good robustness of the new predictive model and its accompanying muscle parameters. More detailed information is published elsewhere (Hwang et al., 2016a). Furthermore, the curved muscle model's improved model performance compared to the straight-line muscle model of a new subject group, whose data were not used to develop both models, could justify the improvements in the quality of complex predicted muscle parameters.

The stable model fidelity of all levels of the curved muscle model indicated that it could precisely predict three-dimensional spinal tissue loads for the entire lumbar spine during complex exertions. In addition, the spine tissue loads for a personalized biologically-assisted curved muscle model have confirmed previous findings that lifting from various load weight, load origin, and load height significantly influenced three-dimensional spine tissue loads. Specifically, lifting heavier objects or lifting from lower height (relative to waist height) significantly increased the magnitude of peak three-dimensional spine tissue loads as noted previously (Davis and Marras, 2000, 2005; Granata et al., 1999; Jorgensen et al., 1999; Marras et al., 2003).

Lifting from increased asymmetric (load origin) positions significantly increased the lateral shear loads, similar to our previous findings (Davis and Marras, 2005; Granata et al., 1999; Marras and Sommerich, 1991). The right or left side muscle forces increased during asymmetric lifting to resist external lateral moments, resulting in greater lateral shear loads. Conversely, the compression and anterior–posterior shear loads tended to decrease with trunk asymmetry, and this trade-off between spinal loads was similar to the results of a previous modelling validation study (Marras and Sommerich, 1991).

It is important to keep in limitations of the present study. First, the curved muscle model was only tested in complex lifting conditions. Validation of other types of occupational tasks such as pushing, pulling, lowering, carrying, and sitting would increase the reliability of the curved muscle model over a variety of different jobs. However, we expect the model to perform well under these conditions given that these exertions are far less complex than the exertions used to assess the model. Second, this model was not tested during exertions that required minimal active exertions and greater passive forces such as lumbar flexion–relaxation. However, the exertions evaluated in this study corresponded to complex exertions observed in occupational settings (Marras et al., 1993).

5. Conclusions

The biologically-assisted curved muscle model examined in this study showed much improved model performance compared to a straight-line muscle model during various complex dynamic lifting exertions. The results indicated good and repeatable model fidelity for the curved muscle model, and indicated that the model was able to reliably predict three-dimensional spinal loads as a function of various external loads and multidimensional lumbar motions during dynamic complex lifting exertions. Collectively, the results suggest that the predicted muscle forces and spinal loads from this model would be acceptable for assessments in complex dynamic occupational environments.

Conflict of interest statement

No potential conflict of interest was reported by the authors.

Acknowledgments

None.

References

Anderson, D.E., D'Agostino, J.M., Bruno, A.G., Manoharan, R.K., Bouxsein, M.L., 2012. Regressions for estimating muscle parameters in the thoracic and lumbar trunk for use in musculoskeletal modeling. J. Biomech. 45, 66–75.
Chaffin, D.B., Redfern, M.S., Erig, M., Goldstein, S.A., 1990. Lumbar muscle size and locations from CT scans of 96 women of age 40 to 63 years. Clin. Biomech. 5, 9–16.
Davis, K.G., Marras, W.S., 2000. Assessment of the relationship between box weight and trunk kinematics: does a reduction in box weight necessarily correspond to a decrease in spinal loading? Hum. Factors 42, 195–208.

Davis, K., Marras, W.S., 2005. Load spatial pathway and spine loading: how does lift origin and destination influence low back response? Ergonomics 48, 1031–1046.
Dufour, J.S., Marras, W.S., Knapik, G.G., 2013. An EMG-assisted model calibration technique that does not require MVCs. J. Electromyogr. Kinesiol. 23, 608–613.
Granata, K.P., Marras, W.S., 1993. An EMG-assisted model of loads on the lumbar spine during asymmetric trunk extensions. J. Biomech. 26, 1429–1438.
Granata, K.P., Marras, W.S., 1995. An EMG-assisted model of trunk loading during free-dynamic lifting. J. Biomech. 28, 1309–1317.
Granata, K.P., Marras, W.S., Davis, K.G., 1999. Variation in spinal load and trunk dynamics during repeated lifting exertions. Clin. Biomech. 14, 367–375.
Hwang, J., Dufour, J.S., Knapik, G.G., Best, T.M., Khan, S.N., Mendel, E., Marras, W.S., 2016a. Prediction of magnetic resonance imaging-derived trunk muscle geometry with application to spine biomechanical modeling. Clin. Biomech. 37, 60–64.
Hwang, J., Knapik, G.G., Dufour, J.S., Aurand, A., Best, T.M., Khan, S.N., Mendel, E., Marras, W.S., 2016b. A biologically-assisted curved muscle model of the lumbar spine: model structure. Clin. Biomech. 37, 53–59.
Jorgensen, M.J., Davis, K.G., Kirking, B.C., Lewis, K.E., Marras, W.S., 1999. Significance of biomechanical and physiological variables during the determination of maximum acceptable weight of lift. Ergonomics 42, 1216–1232.
Jorgensen, M.J., Marras, W.S., Granata, K.P., Wiand, J.W., 2001. MRI-derived moment-arms of the female and male spine loading muscles. Clin. Biomech. 16, 182–193.
Marras, W.S., Sommerich, C.M., 1991. A three-dimensional motion model of loads on the lumbar spine: II. Model validation. Hum. Factors 33, 139–149.
Marras, W.S., Lavender, S.A., Leurgans, S.E., Rajulu, S.L., Allread, W.G., Fathallah, F.A., Ferguson, S.A., 1993. The role of dynamic three-dimensional trunk motion in occupationally-related low back disorders: the effects of workplace factors, trunk position, and trunk motion characteristics on risk of injury. Spine 18, 617–628.
Marras, W.S., Granata, K.P., 1997. The development of an EMG-assisted model to assess spine loading during whole-body free-dynamic lifting. J. Electromyogr. Kinesiol. 7, 259–268.
Marras, W.S., Jorgensen, M.J., Granata, K.P., Wiand, B., 2001. Female and male trunk geometry: size and prediction of the spine loading trunk muscles derived from MRI. Clin. Biomech. Bristol Avon 16, 38–46.
Marras, W.S., Davis, K.G., Jorgensen, M., 2003. Gender influences on spine loads during complex lifting. Spine J. 3, 93–99.
Mirka, G.A., Marras, W.S., 1993. A stochastic model of trunk muscle coactivation during trunk bending. Spine 18, 1396–1409.
Moga, P.J., Erig, M., Chaffin, D.B., Nussbaum, M.A., 1993. Torso muscle moment arms at intervertebral levels T10 through L5 from CT scans on eleven male and eight female subjects. Spine 18, 2305–2309.
Seo, A., Lee, J.-H., Kusaka, Y., 2003. Estimation of trunk muscle parameters for a biomechanical model by age, height and weight. J. Occup. Health 45, 197–201.
Theado, E.W., Knapik, G.G., Marras, W.S., 2007. Modification of an EMG-assisted biomechanical model for pushing and pulling. Int. J. Ind. Ergon. 37, 825–831 Musculoskeletal Load of Push–Pull Tasks.